Author's Accepted Manuscript

www.elsevier.com

Microstructure and electrical properties of co-sputtered Cu embedded amorphous SiC

Junqing Fan, Liudi Jiang, Le Zhong, Robert P. Gowers, Katrina A. Morgan, C.H. de Groot

PII: S0167-577X(16)30645-0
DOI: http://dx.doi.org/10.1016/j.matlet.2016.04.144
Reference: MLBLUE20741

To appear in: *Materials Letters*

Received date: 19 January 2016
Revised date: 31 March 2016
Accepted date: 17 April 2016

Cite this article as: Junqing Fan, Liudi Jiang, Le Zhong, Robert P. Gowers Katrina A. Morgan and C.H. de Groot, Microstructure and electrical propertie of co-sputtered Cu embedded amorphous SiC, *Materials Letters* http://dx.doi.org/10.1016/j.matlet.2016.04.144

Microstructure and electrical properties of co-sputtered Cu embedded amorphous SiC

Junqing Fan[1*], Liudi Jiang[1], Le Zhong[1], Robert P. Gowers[1], Katrina A. Morgan[2], C. H. de Groot[2]

[1]Faculty of Engineering and the Environment, University of Southampton, Southampton, Hampshire SO17 1BJ, United Kingdom

[2]Faculty of Physical Sciences and Engineering, University of Southampton, Southampton, Hampshire SO17 1BJ, United Kingdom

[*]Corresponding author. jf3g12@soton.ac.uk

Abstract

The properties of co-sputtered Cu embedded amorphous SiC were studied. The effect of the microstructure features on the electrical conduction of the SiC films, with Cu volume% between 0% and 57%, was analysed by temperature dependent measurements, along with an effective-medium approximation model. The electrical conduction in Cu embedded amorphous SiC, was attributed to the tunnelling mechanism. Dielectric constants of the Cu embedded amorphous SiC composites were measured from purposely fabricated micro-capacitors using Cu embedded amorphous SiC composites as the dielectric layer, showing a decrease in dielectric constant with increasing Cu volume%. The electrical contacts between metal electrodes, i.e. Cu and Au, and Cu embedded amorphous SiC composites resulted in Schottky emission.

Keywords: Amorphous SiC; Copper nanoparticles; Co-sputter; Schottky emission.

1. Introduction

Cu Nanoparticles (NPs) embedded composites have shown promise for applications in many fields of electronic devices [1, 2], optics [3, 4], ferromagnetism [5, 6] and catalysts [7]. Recently, Cu NPs embedded dielectric materials have also attracted significant interest for non-volatile resistive memory (RM) applications [2, 8]. It was reported that embedding metal NPs in the resistive switching dielectric layers can improve stability in e.g. SiO_2 [2] and TiO_2 [9] based RMs. This is because that well-dispersed metal NPs can enhance local electrical field within the dielectric layer which subsequently lowers operating voltages, and enhances switching stability [9]. In particular, Cu NPs embedment has shown improvement in RM switching behaviour [2], and Cu concentration in the dielectric switching layer alters the materials properties which have a notable effect on the RM devices [10]. From a general materials point of view, it is also important to study the effect of Cu NPs embedded composite films with different Cu concentration.

We chose to study amorphous SiC and Cu (a-SiC:Cu) based composites because a-SiC has recently shown extremely promising properties as a dielectric material for RMs with excellent retention [11], and ultrahigh OFF/ON resistance ratios [12]. Cu has been commonly used as active electrodes for a-SiC based RMs. Despite many studies on Cu NPs embedded thin films, there is no reported result on microstructure and electrical properties of a-SiC:Cu composites. Such studies, especially in below percolation regime, would be beneficial for application areas such as RMs [12] and back end of the line dielectrics [13, 14], which both require the composites to exhibit a high resistive or dielectric state. Systematic studies of the microstructure, electrical and dielectric properties of the composites could potentially provide material insight into these applications.

In this work, a-SiC:Cu thin films were deposited at room temperature by co-sputtering of SiC and Cu targets. Conventional magnetron sputtering was chosen due to its advantages of low cost, room temperature processing, and compatibility with main stream CMOS processes [15-17]. Results suggest that Cu NPs dispersed in a-SiC have been successfully achieved by tuning target power. The microstructures, electrical, and dielectric properties of the deposited a-SiC:Cu composites with different Cu volume% were investigated.

2. Experimental

All a-SiC:Cu thin films in this work were deposited on Si wafers covered with a 1µm thick thermal oxide layer. Co-sputtering from SiC (99.5%) and Cu (99.99%) targets was carried out using RF and DC power supplies, respectively, in a Kurt J. Lesker sputter system. The Cu volume% in the deposited films was controlled by adjusting the value of the RF and DC power. In the context of this paper, Cu% refers to Cu volume%. For all depositions, Argon (gas flow 3sccm) was used as sputtering gas, the chamber pressure was kept at 5×10^{-3}mbar, and deposition duration was 60mins. Substrates were maintained at room temperature. For each deposition, a-SiC:Cu film on an Al substrate was also produced, which was subsequently used to conduct Energy Dispersive X-ray (EDX) spectroscopy in order to extract the Cu% in the films. The use of Al substrates eliminates any possible Si EDX spectra from the SiO_2/Si substrates and thus ensure all Si spectra can be attributed to the deposited a-SiC:Cu layers. Microstructure of the films was studied by X-ray Diffraction (XRD) and Scanning Electron Microscopy (SEM).

A cryogenic probe station with an Agilent B1500A was used to measure electrical resistance of the deposited a-SiC:Cu films as a function of temperature. A range of micro-capacitors with areas ranging from $10\times10\mu m^2$ to $100\times100\mu m^2$ were fabricated using a 40nm thick a-SiC:Cu layers sandwiched between Cu and Au electrodes (Cu/a-SiC:Cu/Au) in order to investigate dielectric properties and conduction mechanism of a-SiC:Cu composites. Detailed fabrication processes of the sandwiched structures were described in [16]. Capacitance of the Cu/a-SiC:Cu/Au micro-capacitors were measured using a HP 4279A CV meter at 0V DC bias. Current density-Voltage (J-V) characteristics were measured using an Agilent B1500A.

3. Results and discussion

Fig. 1a shows EDX spectra and corresponding Cu volume% for a set of a-SiC:Cu samples. a-SiC:Cu layers with Cu% range from 0% to 57% were successfully achieved. Fig. 1b shows high resolution XRD spectra of the composite films with different Cu%. The absence of the characteristic crystalline SiC (111) peak at 35.7^o [18] indicates the sole presence of amorphous SiC in the films. The peak observed at 43.6^o corresponds to Cu NPs [19], and its broadening reflects the Cu NPs diameter (D) according to the Scherrer equation [20],

$$D = 0.94\lambda/[\beta\cos(\theta)] \quad (1)$$

where λ is the X-ray wavelength of the Cu Kα radiation (0.1541nm), β is the full width at half maximum of the peak, and θ is the diffraction angle. Cu NPs sizes of approximately 1.0nm, 1.2nm, 2.0nm, and 2.5nm were obtained for a-SiC:Cu films with 20%, 30%, 46%, and 57% Cu, respectively. The increase of the Cu NPs size with increasing Cu% indicates that higher Cu target power not only affect the Cu% but also increase the Cu NPs sizes. The increase of Cu NPs size with Cu target power aligns with reported works in relation to metal depositions using magnetron sputtering [21, 22]. Generally speaking, high target power induces sputtered species with high energy and thus high mobility on the substrate which subsequently form large particles. Fig. 1c-f show clear increase of a-SiC:Cu surface roughness with Cu%, further indicating the increase of Cu NPs size when higher Cu target power was applied. Uniform morphology is observed for all Cu% from Fig. 1c-f, suggesting that well dispersed Cu NPs were obtained via the co-sputtering depositions.

Fig. 2a shows the normalized resistance R/R_{300K} of typical a-SiC:Cu films as a function of temperature. a-SiC:Cu films with 20%, 30% and 46% Cu show semiconductor-like temperature dependence, where resistance decreases with increasing temperature, while the film with 57% Cu starts to show sign of metal-like electrical behaviour. This suggests that the metallic percolation Cu% (X_c) is approximately at 57%, which is within the percolation thresholds estimated for metal-insulator composites in general [23]. The primary aim of this work is to investigate the electrical properties of the composite with Cu% below the percolation threshold, and Fig. 2b shows room temperature resistivity of all composite films as a function of Cu%.

Since the Cu NPs sizes (<2.5nm) in our films are much smaller than the film thickness (in the range between 120nm to 580nm), the composite films can be assumed to be three dimensional (3D) metal-insulator composites. An effective medium approximation model has recently been reported to evaluate electrical conduction mechanism in 3D metal-insulator composites [23, 24]. In particular, when metal volume% is in the regime below percolation threshold X_c, the resistivity of the composite ρ as function of metal volume% X is dominated by tunnelling conduction mechanism which follows,

$$\frac{(X/X_c)}{\sqrt{1/\Sigma\rho+1}} + 4X\left\{\left[1+\frac{\xi}{2D}ln(\alpha\Sigma\rho+1)\right]^3 - 1\right\} = 1 \qquad (2)$$

where α is a constant signifying ratio of tunnelling conductance over metallic conductance, Σ is a fitting parameter associated with conductivity of the effective medium and has a unit of S/cm, D is the diameter of metal NPs, and ξ is the tunnelling decay length which follows $\xi=\hbar/\sqrt{(2mU_0)}$ where m is the electron mass and U_0 is tunnelling barrier height. ξ value is estimated to be 0.2nm by using U_0=0.94eV for Cu/a-SiC contact [16]. Using ξ=0.2nm, D=2.5nm, and X_c =57% Cu in Eq. (2), an optimal fit with R^2 value of 0.94 is achieved as shown in Fig. 2b with $\alpha=1.7\times10^{-4}$ and $\Sigma=2.5\times10^{5}$S/cm. This confirms that, for a-SiC:Cu composites, when Cu is below its percolation threshold, tunnelling plays an important role in its electrical conduction performance.

The dielectric constants of a-SiC:Cu composites were obtained by measuring capacitance of typical Cu/a-SiC:Cu/Au micro-capacitors, as shown in Fig. 3. Inset of Fig. 3 shows a cross-section SEM image of a typical Cu/a-SiC:Cu/Au micro-capacitor with the middle dielectric layer of 40nm thickness. Dielectric constant ε_r was extracted as 7.5, 5.4, and 4.6, for a-SiC:Cu with 0%, 20%, and 30% Cu, respectively. In particular, ε_r=7.5 for pure a-SiC aligns well with previous reported value [25].

J-V characteristics were measured by applying voltage to the Cu electrode while keeping Au electrode always grounded as shown in Fig. 3 inset, in order to investigate the conduction mechanism at the interface between metal electrodes and a-SiC:Cu composites. Fig. 4a and 4b show Ln(J)- √ V when applying negative (-V) and positive (+V) voltage to the Cu electrode, respectively. Linear fits are obtained for both voltage polarities which suggest Schottky emission mechanism following [26],

$$J = A^{*}T^{2}exp(\frac{-q\phi_{B}}{kT} + \frac{q}{kT}\sqrt{\frac{qE}{4\pi\varepsilon}}) \quad (3)$$

where A^{*} is the Richardson constant, T is the temperature, ϕ_B is the Schottky Barrier Height (SBH), E is electrical field, k is the Boltzmann constant, ε is permittivity of the dielectric layer. Zero bias SBH values of 0.91eV, 0.90eV and 0.85eV are extracted for 0%, 20%, and 30% Cu, respectively. The SBHs decrease with increasing Cu% is possibly related to enhanced tunnelling conduction mechanism [27] in a-SiC:Cu composites with higher Cu%. Furthermore, symmetric characteristic of Ln(J)- √ V is observed in the –V and +V regions for all the devices. Despite the work function difference between Cu (4.9eV) and Au (5.3eV), SBH values in both voltage polarity regimes are similar. This may relate to strong Fermi level pinning effect in SiC due to the existence of defects [28] and high degree of covalency [25], which play a dominating effect in determining the SBHs.

4. Conclusions

Cu NPs embedded a-SiC films with controlled Cu% were deposited by co-sputtering process. Cu NPs diameters up to approximately 2.5nm were extracted from high resolution XRD spectra. Electrical resistance vs temperature suggests that the percolation threshold is close to 57% Cu. Below the percolation threshold, tunnelling is identified as the key conduction mechanism of the composites with the resistivity well described by the effective medium approximation model. Measurements from Cu/a-SiC:Cu/Au micro-capacitors give dielectric constants of 7.5, 5.4, and 4.6 for a-SiC:Cu with 0%, 20%, and 30% Cu, respectively. Further J-V analysis suggests that both Cu and Au contacts with the a-SiC:Cu exhibit Schottky emission conduction mechanism and SBHs up to 0.91eV were obtained. Symmetric characteristics also suggest that Fermi level pinning effect may play a key role in the determination of the SBHs at metal/a-SiC interfaces. Thus, this work provides a systematic study on microstructure and electrical properties of co-sputtered Cu embedded amorphous SiC materials. New findings include determination of electrical conduction mechanism, dielectric constants and metal contact conduction mechanism of a-SiC:Cu, especially in relation to different Cu% and corresponding microstructures in the below percolation regime. These are the key material properties for potential applications of a-SiC:Cu in fields such as resistive memory devices, back end of the line dielectric etc. Thus, the exploitation of the results could underpin new device designs and developments.

Acknowledgments

We (Katrina. A. Morgan and C. H. de Groot) thank the EPSRC for support (EP/J002968/1). We also would like to thank Dr. Shuncai Wang, from University of Southampton, for his help with SEM. All data supporting this study are openly available from the University of Southampton repository at http://dx.doi.org/10.5258/SOTON/388275.

References

[1] R.K. Gupta, D.Y. Kusuma, P.S. Lee, M.P. Srinivasan, Mater. Lett. 68 (2012) 287-289.

[2] C.Y. Liu, J.J. Huang, C.H. Lai, C.H. Lin, Nanoscale Res. Lett. 8 (2013) 156.

[3] Y. Takeda, C.G. Lee, V.V. Bandourko, N. Kishimoto, Mater. Trans. 43 (2002) 1057-1060.

[4] Y. Takeda, J.P. Zhao, C.G. Lee, V.T. Gritsyna, N. Kishimoto, Nucl. Instrum. Methods Phys. Res., Sect. B 166 (2000) 877-881.

[5] J.S. Garitaonandia, M. Insausti, E. Goikolea, M. Suzuki, J.D. Cashion, N. Kawamura, et al., Nano Lett. 8 (2008) 661-667.

[6] C. Zhao, C. Zhen, Y. Li, L. Ma, C. Pan, D. Hou, Solid State Commun. 152 (2012) 752-756.

[7] H. Wang, Y. Huang, Z. Tan, X. Hu, Anal. Chim. Acta 526 (2004) 13-17.

[8] S.P. Thermadam, S.K. Bhagat, T.L. Alford, Y. Sakaguchi, M.N. Kozicki, M. Mitkova, Thin Solid Films 518 (2010) 3293-3298.

[9] W.Y. Chang, K.J. Cheng, J.M. Tsai, H.J. Chen, F. Chen, M.J. Tsai, et al., Appl. Phys. Lett. 95 (2009) 042104.

[10] C.Y. Liu, Y.H. Huang, J.Y. Ho, C.C. Huang, J. Phys. D: Appl. Phys. 44 (2011) 205103.

[11] W. Lee, J. Park, M. Son, J. Lee, S. Jung, S. Kim, et al., IEEE Electron Device Lett. 32 (2011) 680-682.

[12] L. Zhong, P.A. Reed, R. Huang, C.H. de Groot, L. Jiang, Solid-State Electron. 94 (2014) 98-102.

[13] S.W. King, M. French, M. Jaehnig, M. Kuhn, B. Boyanov, B. French, J. Vac. Sci. Technol. B 29 (2011) 051207.

[14] S.W. King, J. Bielefeld, G. Xu, W.A. Lanford, Y. Matsuda, R.H. Dauskardt, et al., J. Non-Cryst. Solids 379 (2013) 67-79.

[15] K. Sasaki, T. Tsutsumi, N. Takada, Jpn. J. Appl. Phys. 50 (2011) 08KE05.

[16] L. Zhong, P.A. Reed, R. Huang, C.H. de Groot, L. Jiang, Microelectron. Eng. 119 (2014) 61-64.

[17] K.A. Honer, G.T.A. Kovacs, Sensors and Actuators A: Physical 91 (2001) 386-397.

[18] M. Kanaya, J. Takahashi, Y. Fujiwara, A. Moritani, Appl. Phys. Lett. 58 (1991) 56-58.

[19] R. Zhou, X. Wu, X. Hao, F. Zhou, H. Li, W. Rao, Nucl. Instrum. Methods Phys. Res., Sect. B 266 (2008) 599-603.

[20] A.L. Patterson, Phys. Rev. 56 (1939) 978-982.

[21] S. Terauchi, N. Koshizaki, H. Umehara, Nanostruct. Mater. 5 (1995) 71-78.

[22] A. Roy, M. Komatsu, K. Matsuishi, S. Onari, J. Phys. Chem. Solids 58 (1997) 741-747.

[23] C. Grimaldi, Phys. Rev. B 89 (2014) 214201.

[24] G. Ambrosetti, I. Balberg, C. Grimaldi, Phys. Rev. B 82 (2010) 134201.

[25] L.M. Porter, R.F. Davis, Mater. Sci. Eng., B 34 (1995) 83-105.

[26] S.M. Sze, K.K. Ng. Physics of semiconductor devices 3rd edition. John Wiley & Sons, Inc; Hoboken, New Jersey, 2007.

[27] J.M. Shannon, Solid-State Electron. 19 (1976) 537-543.

[28] D.J. Ewing, L.M. Porter, Q. Wahab, X. Ma, T.S. Sudharshan, S. Tumakha, et al., J. Appl. Phys. 101 (2007) 114514.

Fig. 1. (a) EDX spectra and (b) XRD spectra of co-sputtered a-SiC:Cu films. SEM images of typical a-SiC:Cu films with (c) 0 Cu%, (d) 20 Cu%, (e) 46 Cu%, and (f) 57 Cu%, respectively.

Fig. 2. (a) Normalized resistance of typical a-SiC:Cu films with different Cu% as a function of temperature, (b) Resistivity of a-SiC:Cu films as a function of Cu% with the solid line showing fit based on effective medium approximation model.

Fig. 3. Capacitance as a function of micro-capacitor device areas. The inset shows a SEM cross-section image of a typical device.

Fig. 4. Ln(J)- $\sqrt{V}$ when applying (a) -V and (b) +V to Cu electrodes.

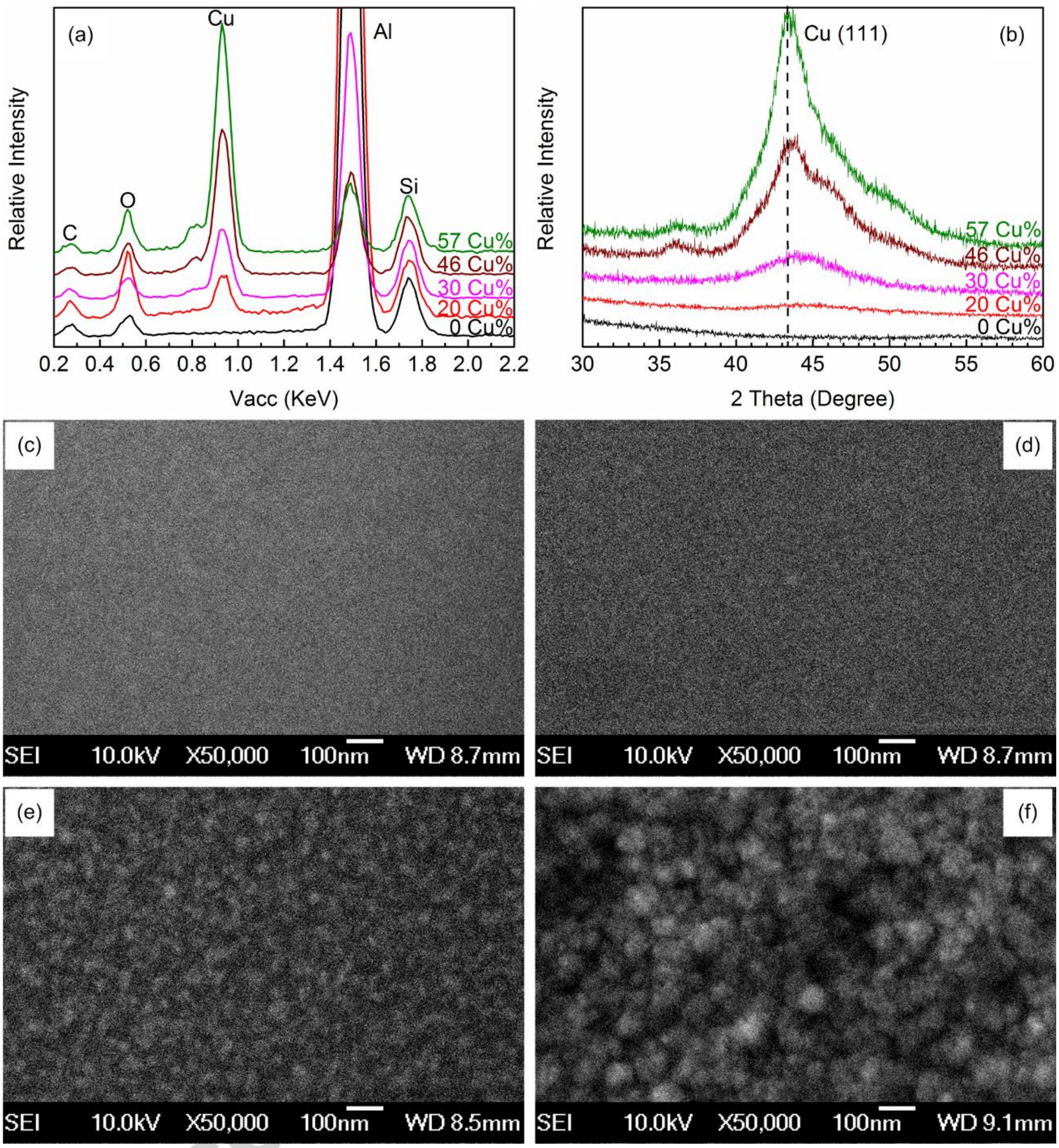
(a)
Cu
Al
C
O
Si
Relative Intensity
57 Cu%
46 Cu%
30 Cu%
20 Cu%
0 Cu%
0.2 0.4 0.6 0.8 1.0 1.2 1.4 1.6 1.8 2.0 2.2
Vacc (KeV)
(b)
Cu (111)
Relative Intensity
57 Cu%
46 Cu%
30 Cu%
20 Cu%
0 Cu%
30 35 40 45 50 55 60
2 Theta (Degree)
(c)
SEI 10.0kV X50,000 100nm WD 8.7mm
(d)
SEI 10.0kV X50,000 100nm WD 8.7mm
(e)
SEI 10.0kV X50,000 100nm WD 8.5mm
(f)
SEI 10.0kV X50,000 100nm WD 9.1mm

Figure 1

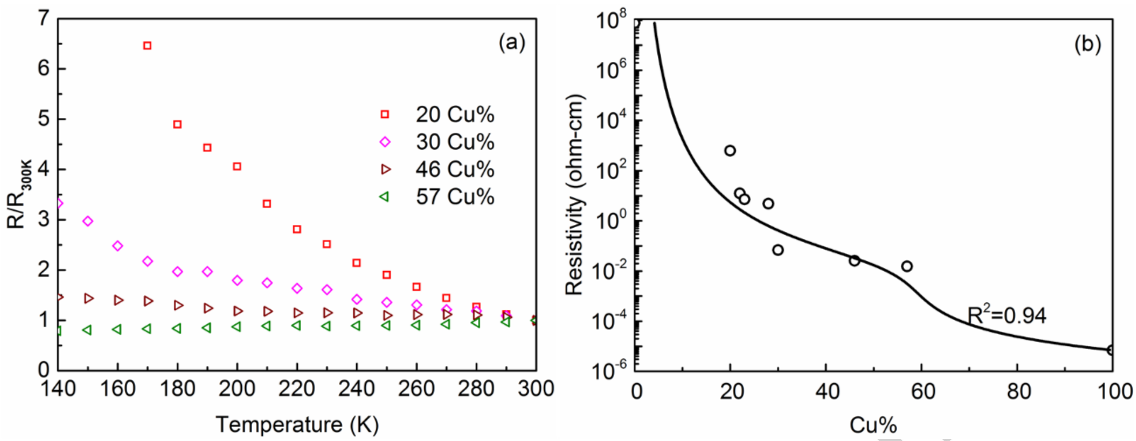
(a)
20 Cu%
30 Cu%
46 Cu%
57 Cu%
R/R300K
Temperature (K)
(b)
Resistivity (ohm-cm)
R2=0.94
Cu%

Figure 2

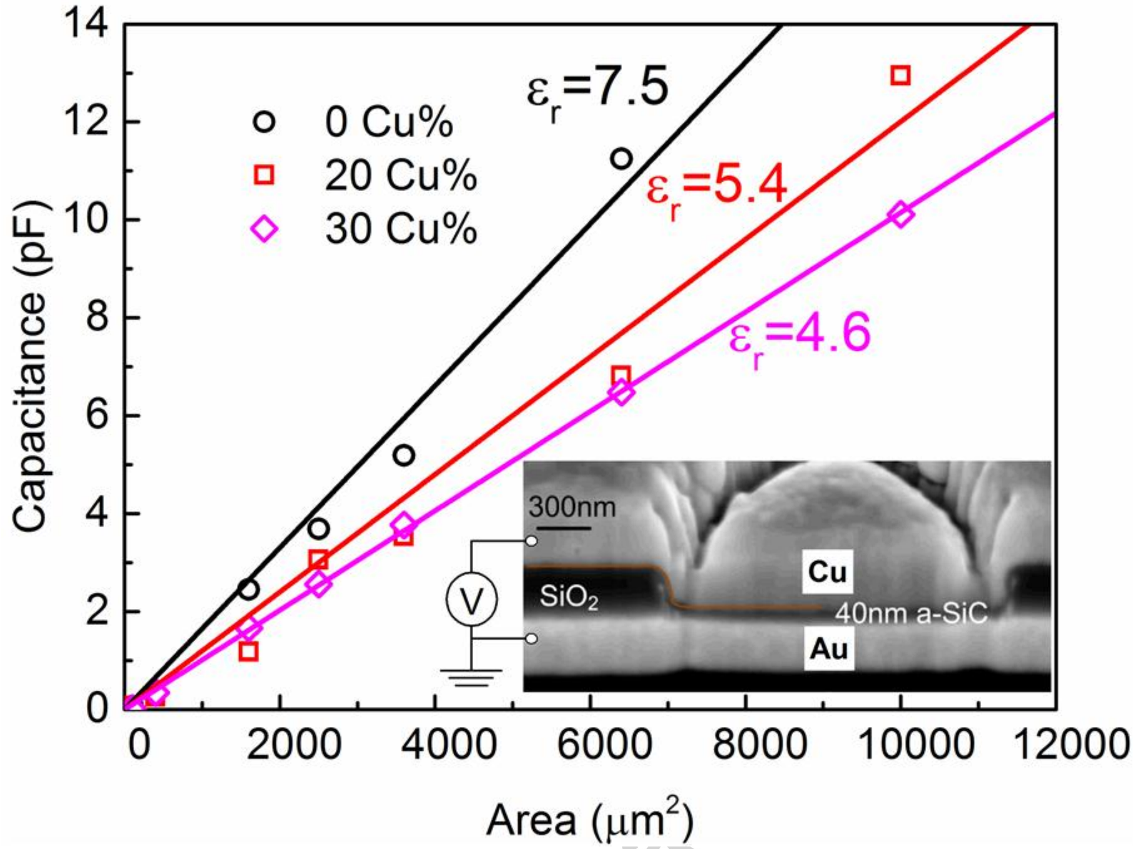
14
12
10
8
6
4
2
0
Capacitance (pF)
0 Cu%
20 Cu%
30 Cu%
εr=7.5
εr=5.4
εr=4.6
300nm
V
SiO2
Cu
40nm a-SiC
Au
0
2000
4000
6000
8000
10000
12000
Area (μm2)

Figure 3

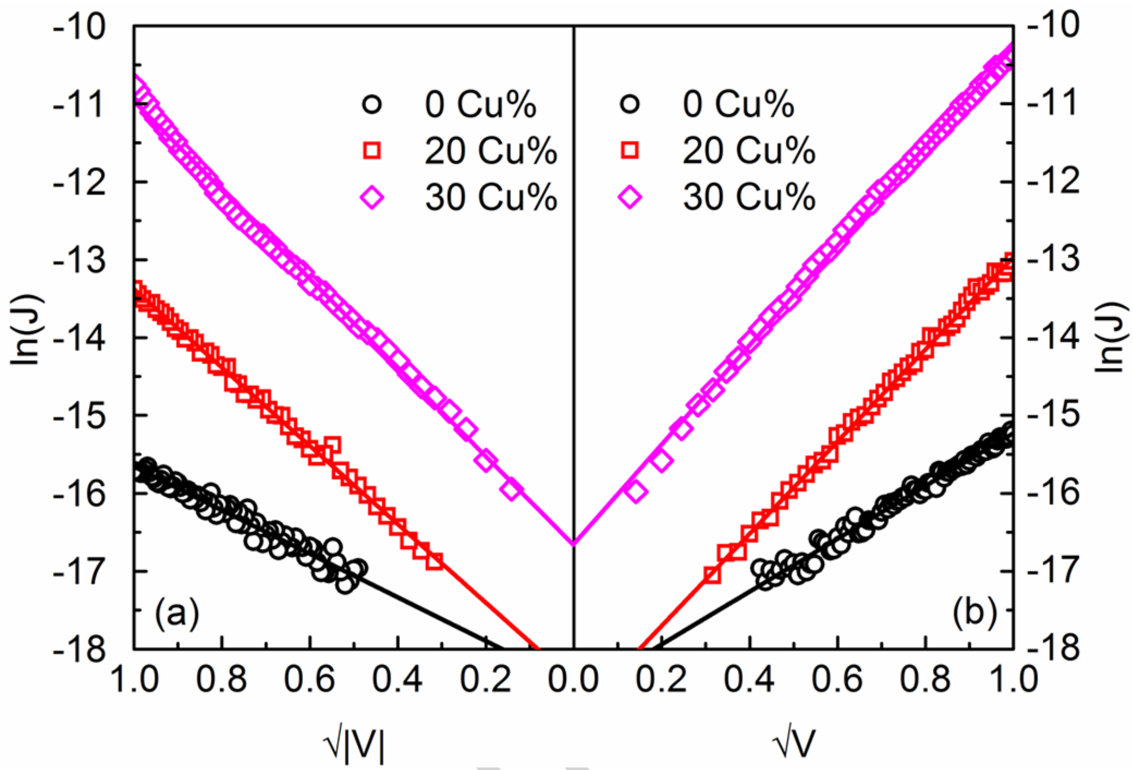

Figure 4

Highlights

- Cu embedded a-SiC composites with Cu nanoparticles sizes up to 2.5nm were obtained.

- Electrical conduction follows the effective medium model in below percolation regime.
- Dielectric constants of a-SiC:Cu composites were measured to be 4.6~7.5.
- Metal/a-SiC:Cu contacts are described by Schottky emission with Fermi level pinning.